Journal of Solid State Chemistry **159,** 204–208 (2001)
doi:10.1006/jssc.2000.9152, available online at http://www.idealibrary.com on IDEAL®

Magnetic Properties of Perovskite $GdCrO_3$

K. Yoshii

Japan Atomic Energy Research Institute (JAERI), Mikazuki, Hyogo 679-5148, Japan

Received January 3, 2001; in revised form March 7, 2001; accepted March 15, 2001; published online May 11, 2001

The gadolinium orthochromate $GdCrO_3$ exhibits negative magnetization when magnetization–temperature curves are measured in a field-cooled mode with low applied fields ($< \sim 500$ Oe). This compound shows canted-antiferromagnetic order of Cr^{3+} moments with a Neel temperature (T_N) of ~ 170 K. With cooling the samples below T_N, magnetization exhibits peak values (M_{MAX}) with a positive sign at ~ 160 K. Below this temperature, it decreases with decreasing temperature, passes through a zero value ($M = 0$) at $T_1 < \sim 130$ K, and continues to decrease until T_{MIN} ($> \sim 25$ K). This behavior is interpreted in connection with the paramagnetic Gd^{3+} moments whose direction is opposite to that of canted Cr^{3+} moments. The maximum absolute value of the negative magnetization was much larger than M_{MAX}, i.e., nearly 30 times as large as M_{MAX} with an applied field of 100 Oe. With further cooling, the magnetization increase and cross again $M = 0$ around T_2 ($> \sim 10$ K).

Key Words: **perovskite; chromium oxide; negative magnetization (reversal of magnetization).**

1. INTRODUCTION

Perovskite chromium oxides $LnCrO_3$ (*Ln*: lanthanides) have the orthorhombic perovskite structure at room temperature (space group *Pbnm*). They exhibit so-called canted-antiferromagnetic order of localized Cr^{3+} moments ($3d^3$, $\mu_{eff} = 3.87\ \mu_B$ for a spin-only value) with Neel temperatures (T_N) of 112–282 K (1–7). The order for one of such compounds, $GdCrO_3$, was reported to take place at 170 K (1, 7). From the magnetic structures for the other $LnCrO_3$ compounds determined from neutron diffraction, the magnetic structure is expected to be a G_xF_z-type configuration (7). Magnetic interactions in this compound were discussed in detail based on the measurements of magnetization–magnetic field (M–H) isotherm curves on a single-crystal (7). It was found that below T_N, a net magnetic moment (canted moment) of Cr^{3+} lies parallel to a crystallographic c axis (i.e., F_z). An antisymmetric exchange interaction or a psudodipolar interaction between Gd and Cr produces an effective magnetic field at the Gd^{3+} ($4f^7$, $\mu_{eff} = 7.94\ \mu_B$ (8)) site, whose direction is opposite to that of the canted Cr^{3+} moments, F_z. This situation is different from those in many perovskites where the directions of the Ln^{3+} moments are perpendicular or parallel to the canted moments (1, 9). The interaction becomes increasingly important at lower temperatures, leading to a spin-reorientation of Cr^{3+} from G_xF_z to G_zF_x around 7 K. In the latter configuration, the net Cr^{3+} moment lies parallel to the crystallographic a axis (i.e., F_x). At lower temperatures, a magnetic interaction between Gd becomes significant, which results in the order of the Gd^{3+} moments at 2.3 K (7).

Recently, the authors have reported negative magnetization (reversal of magnetization) below ~ 140 K for an isostructural compound $La_{0.5}Pr_{0.5}CrO_3$ ($T_N \sim 260$ K), which is a solid solution between $LaCrO_3$ ($T_N \sim 288$ K) and $PrCrO_3$ ($T_N \sim 240$ K) (10). This effect is observed for magnetization–temperature (M–T) curves in field-cooled measurements with low applied fields ($< \sim 5000$ Oe) and has not been observed for the end compounds. The maximum absolute value of the negative magnetization (at 2 K) is ~ 40 times as large as that of positive magnetization (at ~ 220 K). Qualitatively, this phenomenon was assumed to arise from the same type of magnetic interaction as in $GdCrO_3$, i.e., opposite direction of the Pr^{3+} moments ($\mu_{eff} = 3.62\ \mu_B$ (8)) to that of the canted Cr^{3+} moment. This experimental result leads to the expectation for the same phenomenon also in $GdCrO_3$. However, to the author's knowledge, its M–T curves have not been reported with low magnetic fields, where the phenomenon is plausibly expected from the behavior of $La_{0.5}Pr_{0.5}CrO_3$. This paper presents the results obtained from DC magnetization measurements.

2. EXPERIMENTAL PROCEDURES

The samples have been prepared in air by solid-state reaction, as in the preparation for $LnCrO_3$ (*Ln*: lanthanides) and $La_{1-x}Nd_xCrO_3$ (3, 4, 6). The starting materials were Gd_2O_3 (4N, Soekawa) and Cr_2O_3 (4N, Soekawa). The initial mixtures were well ground, pelletized and fired in air at 1400°C for 24 h. This firing was repeated two to three times. Three samples were prepared, and were verified to show

0022-4596/01 $35.00

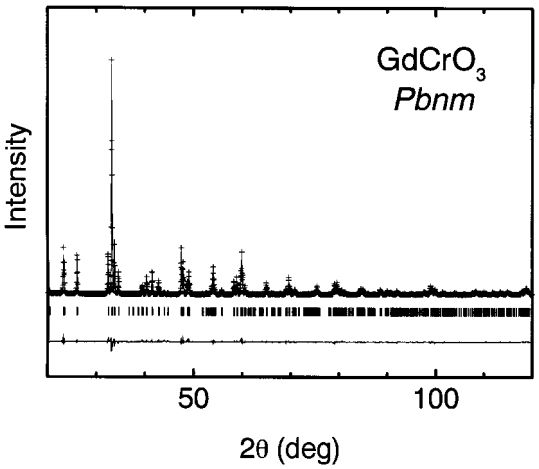

FIG. 1. XRD patterns at room temperature for $GdCrO_3$. The observed and calculated patterns are shown as the cross markers and the top solid line, respectively. The vertical markers stand for the angles of calculated Bragg reflections. The lowest solid line represents the difference between the calculated and observed intensities. The fit was done assuming the space group *Pbnm*. The parameters obtained are $a = 5.3142(1)$, $b = 5.5239(1)$, and $c = 7.6063(1)$ Å, $R_{wp} = 13.77\%$, $R_p = 9.83\%$, $Re = 8.86\%$, and $R_F = 4.34\%$. The other parameters such as atomic positions are essentially the same as those for $LaCrO_3$ (3).

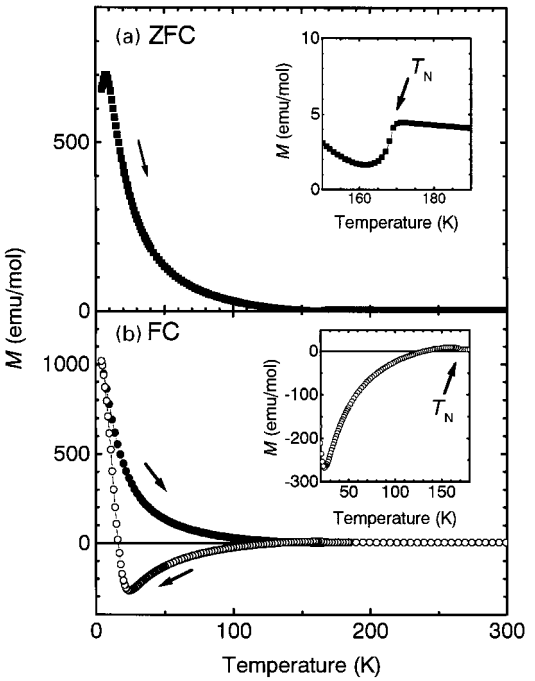

FIG. 2. (a) ZFC and (b) FC M–T curves for $GdCrO_3$ with an applied field of $H = 100$ Oe. In (b), filled (●) and open (○) circles stand for FC(H) and FC(C) modes, respectively. See experimental details in text.

reproducible structural and magnetic properties. The crystal structure was determined by powder XRD (X-ray diffraction) measurements using Cu$K\alpha$ radiation (MAC Science Co., M03XHF^{22}) with an angle (2θ) step of 0.04° between $2\theta = 20$ and 120°. The XRD patterns were verified to consist only of the reaction products and were analyzed by the Rietveld method using the program RIETAN (11, 12). They are shown in Fig. 1. The lattice parameters are $a = 5.3142(1)$, $b = 5.5239(1)$, and $c = 7.6063(1)$ Å with the space group *Pbnm*, which are close to those reported previously, $a = 5.312$, $b = 5.514$, and $c = 7.611$ Å (7) (see this reference for the crystal structure). DC magnetization measurements were performed with a SQUID magnetometer (Quantum Design MPMS). Magnetization–temperature (M–T) curves were measured between 4.5 and 400 K in field-cooled (FC) and zero-field cooled (ZFC) modes with an applied field (H) between 20 and 10,000 Oe. As the lowest measurement temperature in the present apparatus is around 2 K, the measurement of the magnetic order of Gd^{3+} at 2.3 K was not the aim of this study. A susceptibility χ is defined as the value of M/H. Magnetization-field (M–H) isotherm curves were measured within $H = \pm 50000$ Oe at representative temperatures.

3. RESULTS AND DISCUSSION

Figure 2 shows the M–T curves for $GdCrO_3$, measured with $H = 100$ Oe. Figure 2a shows that the ZFC curve exhibits a maximum of magnetization at ~8 K. Since this temperature is close to that for the spin-reorientation temperature of ~7 K, the behavior can be ascribed to the rotation of magnetic moments or magnetic domains, each of which has a random orientation after zero-field cooling. The magnetization monotonically decreases with heating and exhibits the antiferromagnetic transition around $T_N \sim 170$ K (inset). The region above T_N obeyed the Curie–Weiss law, $1/\chi = (1/C)(T - \theta)$. The paramagnetic moment calculated from the C value was close (~95%) to that estimated from the contribution of a spin-only Cr^{3+} and a free-ion Gd^{3+} moments. A Weiss temperature θ obtained is antiferromagnetic, ~ -35 K.

Figure 2b shows the two FC curves. One was measured on heating the sample with $H = 100$ Oe after field-cooling (filled circles). This mode will be denoted as the FC(H) mode hereafter. The profile of this curve is analogous to that of the ZFC curve in Fig. 2a, except for the absence of the magnetization peak around 8 K. The difference of magnetization below this temperature is attributed to magnetic order. The other curve was measured on cooling the sample with the applied field of 100 Oe (open circles). This process will be denoted as the FC(C) mode hereafter. The canted-antiferromagnetic transition is observed at $T_N \sim 170$ K (inset), where the net canted Cr^{3+} moment lies parallel to the c axis as noted (7). The magnetization shows a peak value (M_{MAX}) of ~9.5 emu/mol around 160 K. Upon further cooling, it decreases again, crosses a zero value at the compensation temperature of $T_1 \sim 130$ K, and exhibits a further decrease

down to $M_{MIN} \sim -270$ emu/mol at $T_{MIN} \sim 25$ K. This magnetization corresponds to $\sim 0.04\ \mu_B$/unit formula. Due to this effect, the FC(H) and FC(C) curves significantly deviate from each other. The negative magnetization means that its direction is opposite to that of the applied field. Thus the system is not obviously in a thermal-equilibrium state. It is interesting that the absolute value of M_{MIN} is much larger than M_{MAX} as was also found for $La_{0.5}Pr_{0.5}CrO_3$ (10); i.e., it is nearly 30 times as large as M_{MAX} in the present case. Considering the effective field at the Gd^{3+} site (7), this behavior is assumed to originate from the opposite direction of the Gd^{3+} moments to the net Cr^{3+} moment. The shape of the curve above T_{MIN} is very similar to that for $La_{0.5}Pr_{0.5}CrO_3$ (10), implying the same origin for both phenomena. Figure 3 shows magnetization measured as a function of time with $H = 100$ Oe just after the FC(C) process down to 30 K. It changes slightly by $\sim 0.5\%$ during ~ 2 days ($\sim 2 \times 10^6$ s). Therefore, the negative magnetizations around T_{MIN} are almost stable during this time span, though this state is not in a true equilibrium.

The upturn of magnetization below $T_{MIN} \sim 25$ K is also a characteristic feature of the FC(C) curve (Fig. 2b). A possible explanation for this behavior is the rotation of the Cr^{3+} moment in the a–c plane (7). Under a zero magnetic field, this rotation manifest itself as a spin-reorientation at ~ 7 K (7), where the G_zF_x mode is induced; i.e., the net Cr^{3+} moment is parallel to the a axis. Continuous rotation is brought about at higher temperatures by applying the external fields (7). With increasing the field, the rotation continues to occur until the field is increased to ~ 2000 Oe where the spin configuration changes also to G_zF_x (7). From this fact, the present upturn is assumed to be brought about by slight rotation of the moments arising from the low applied field. For $La_{0.5}Pr_{0.5}CrO_3$, the FC(H) and FC(C) curves were found to almost trace below T_N in low applied fields ($< \sim 1000$ Oe) (10). This is in agreement with no apparent additional transition in $La_{0.5}Pr_{0.5}CrO_3$ below T_N (~ 260 K) (10). With further cooling, the magnetization

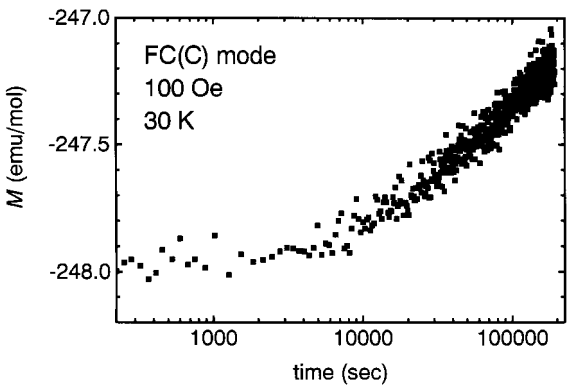

FIG. 3. Magnetization (M) plotted as a function of time with $H = 100$ Oe at 30 K after FC(C) process.

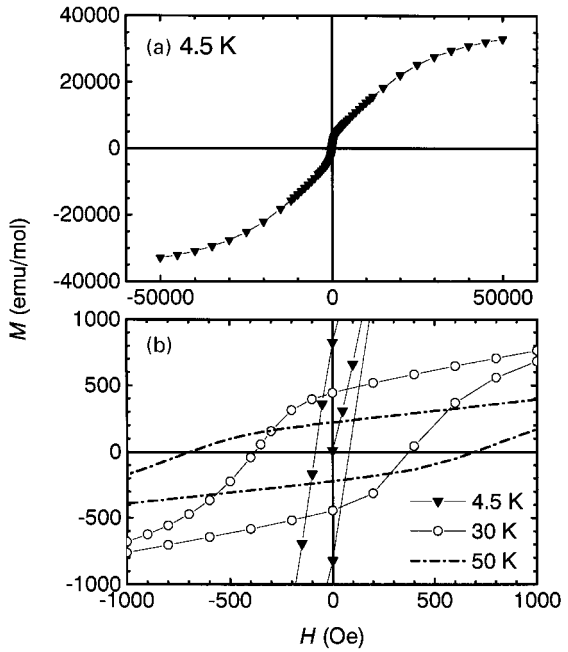

FIG. 4. M–H curves for $GdCrO_3$ measured at (a) 4.5 K and (b) 4.5, 30, and 50 K.

increases again and crosses a zero value ($M = 0$) at the second compensation temperature of $T_2 \sim 17$ K (Fig. 2b). In this experiment, though the measured magnetization is spatially averaged in the polycrystalline sample, it can be essentially considered that the applied field has the same direction as that of the net canted Cr^{3+} moment observed between T_{MIN} and T_N, which is parallel to the c axis. If the spin configuration is perfectly changed to G_zF_x around T_2, and the Cr^{3+} and Gd^{3+} moments have antiparellel coupling, the net Cr^{3+} and Gd^{3+} moments are perpendicular to the c axis. Therefore, magnetization could exhibit a zero value. The temperature of T_2 is higher than the spin-reorientation temperature at a zero field of ~ 7 K. This might be because the rotation to the G_zF_x mode is promoted by the applied field. The further upturn of magnetization below T_2 might be related to the order of Gd^{3+} at 2.3 K (7).

Figure 4 shows the M–H curves at several temperatures. Figure 4a shows that perfect saturation is not established with $H = 50000$ Oe at 4.5 K. From the M–H curve measurements at various temperatures, it was also found that a coercivity exhibited a maximum (~ 900 Oe) around 70 K, and tended to monotonically decrease below 30 K with decreasing temperature. This is demonstrated in Fig. 4b. The result implies that the rotation of the Cr^{3+} moments occurs more easily below ~ 30 K because of the reduction of anisotropy, and it suggests also a possible change of a crystallographic or electronic structure below T_{MIN} which has not been reported yet. Further studies are needed to clarify more details of these behavior observed below T_{MIN}.

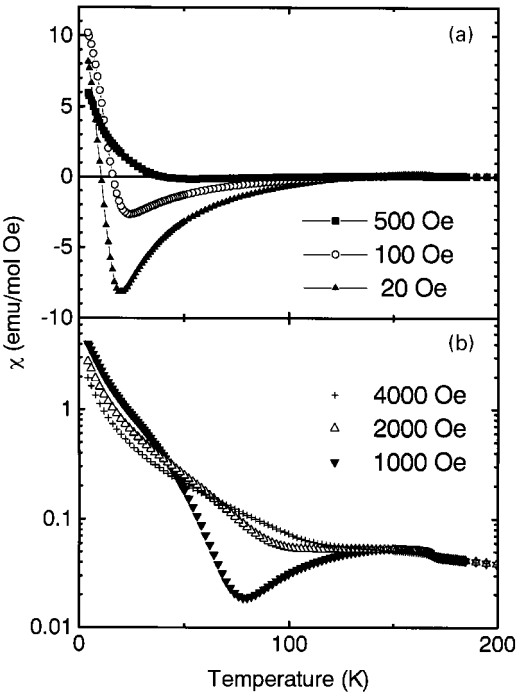

FIG. 5. χ–T curves for $GdCrO_3$ with several different applied fields, measured in FC(C) mode.

Figure 5 shows the χ–T curves measured in the FC(C) mode with some representative applied fields between 20 and 4000 Oe. The results in the FC(H) measurements were essentially identical to that in Fig. 2b. It is evident that the absolute values of negative susceptibility below T_N monotonically decreases with increasing the applied field (H), plausibly because of the increase in the Zeeman energy of the field. With $H \geq 1000$ Oe, no negative susceptibility (magnetization) is observed in the whole temperature region. The monotonic increase in T_{MIN} and T_2 with increasing H indicates that the spin-reorientation is assisted by the magnetic field as noted. The measurements were performed in fields up to 10000 Oe. The results were analogous to that with $H = 4000$ Oe.

The normal behavior of magnetic materials is that the FC magnetization has the same direction as the applied field and lies above the ZFC magnetization. Distinct negative magnetization has been reported only for a few systems other than $La_{0.5}Pr_{0.5}CrO_3$ such as a perovskite $LaVO_3$ (13–15) and a ferrimagnetic spinel $Co[CoV]O_4$ (16). The compensation temperatures are $\sim$110–140 K and $\sim$70 K for the former and latter systems, respectively. The behavior for $LaVO_3$ was interpreted in connection with the enhancement of an orbital moment of V^{3+}, which is brought about by the magnetostriction below $T_N = 142$ K (15). For $Co[CoV]O_4$, it was attributed to different temperature dependence of inequivalent magnetic sublattices (16). This situation is qualitatively the same as in $GdCrO_3$ having two inequivalent magnetic sublattices of Cr^{3+} and Gd^{3+}, which are coupled antiferromagnetically due to the internal field of Cr^{3+}.

From the analysis of the M–H curves measured at various temperatures (7), it was proposed that the measured moment **M** for $GdCrO_3$ above the spin-reorientation temperature could be expressed as:

$$\mathbf{M} = \mathbf{M}_{Cr} + C(\mathbf{H}_I + \mathbf{H})/(T - \theta). \quad [1]$$

Here, $\mathbf{M}_{Cr}$, C, $\mathbf{H}_I$, $\mathbf{H}$, and θ stand for the canted moment of Cr^{3+}, a Curie constant, an internal field from Cr^{3+}, an applied field and a Weiss temperature, respectively. The Curie constant C was fixed to be that calculated from the free Gd^{3+} moment. If the applied field (**H**) is along the c axis (i.e., parallel to the net canted Cr^{3+} moment), its direction is opposite to $\mathbf{H}_I$. Thus, the relationship of $\mathbf{M} = \mathbf{M}_{Cr}$ is satisfied below T_N when **H** is equal to $-\mathbf{H}_I$. Using this fact, the values of $\mathbf{M}_{Cr}$, $\mathbf{H}_I$ and θ were calculated as 400 emu/mol, -5500 Oe, and -2.3 K, respectively (7). It was found that this proposed formula could be applied also to the present M–T curve data between $\sim T_{MIN}$ and $\sim$150 K, as shown in Fig. 6. The suitable fit without considering temperature dependence of $\mathbf{M}_{Cr}$ is because the magnetic effect of the large Gd^{3+} moment far overcomes that of the small canted Cr^{3+} moment. The values of $\mathbf{M}_{Cr}$, $\mathbf{H}_I$ and θ obtained are $\sim$100 emu/mol, ~ -1900 Oe, ~ -13 K, respectively. These were found to be close to those estimated from similar M–H curve analyses (in the region of $H > \sim 500$ Oe) to that noted in Ref. (7). The absolute values of $\mathbf{M}_{Cr}$ and $\mathbf{H}_I$ smaller than the above-described values (7) are plausibly due to the spatial average of magnetization in the polycrystalline sample. For the other samples and other applied fields ($\leq$500 Oe), the same formula could be applied with different parameter values indicating their field dependence in a low field region: $\mathbf{M}_{Cr}$, $\mathbf{H}_I$ and θ were $\sim$50–100 emu/mol,

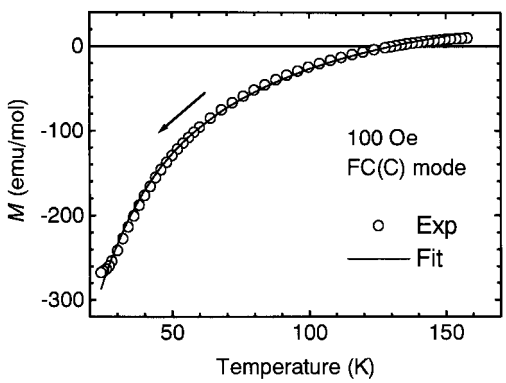

FIG. 6. M–T curves for $GdCrO_3$ with $H = 100$ Oe. Experimental data taken in FC(C) mode is labeled as Exp. Solid line represents a Curie–Weiss-type fit for Gd^{3+} moment. Further details are in text.

~ -1000–1900 Oe, ~ -13–0 K, respectively. The present $\mathbf{H}_I$ value is consistent with the fact that the susceptibilities (magnetization) below T_N show no decrease with decreasing temperature for $\mathbf{H} \geq 2000$ Oe as seen in Fig. 5, because the direction of $\mathbf{H}_I + \mathbf{H}$ is no longer opposite to $\mathbf{M}_{Cr}$. From these results, essentially, it can be concluded that the negative magnetization above T_{MIN} is not due to an additional magnetic phase transition, but due to the paramagnetic effect of Gd^{3+}. The same formula could be applied also to $La_{0.5}Pr_{0.5}CrO_3$; its details will be published together with neutron diffraction data and magnetic data of $La_{1-x}Pr_xCrO_3$, whose measurements are currently under way.

REFERENCES

1. J. B. Goodenough and J. M. Longo, *in* "Landolt-Bornstein, Group III, Vol. 4: Magnetic and Other Properties of Oxides and Related Compounds," p. 126. Springer-Verlag, New York, 1970.
2. S. Nomura, *in* "Landolt–Bornstein, Group III, Vol. 12: Magnetic and Other Properties of Oxides and Related Compounds," p. 368. Springer-Verlag, New York, 1978.
3. C. P. Khattak and D. E. Cox, *Mater. Res. Bull.* **12,** 463 (1977).
4. T. Arakawa, S. Tsuchi-ya, and J. Shiokawa, *Mater. Res. Bull.* **16,** 97 (1981).
5. E. F. Bertaut, J. Mareschal, G. de Vries, R. Aleonald, R. Pauthenet, J. P. Rebouillat, and V. Zarubicka, *IEEE. Trans. Mag.* **2,** 453 (1966).
6. H. Taguchi, M. Nagao, and Y. Takeda, *J. Solid State Chem.* **114,** 236 (1995) (doi:10.1006/jssc.1995.1034).
7. A. H. Cooke, D. M. Martin, and M. R. Wells, *J. Phys. C*: *Solid State Phys.* **7,** 3133 (1974).
8. J. H. Van Vleck, "The Theory of Electric and Magnetic Susceptibilities." Oxford University Press, London, 1965.
9. H. C. Nguyen and J. B. Goodenough, *J. Solid State Chem.* **119,** 24 (1995).
10. K. Yoshii and A. Nakamura, *J. Solid State Chem.* **155,** 447 (2000) (doi:10.1006/jssc.2000.8943).
11. F. Izumi, "The Rietveld Method" (R. A. Young, Ed.), Chap. 13. Oxford University Press, London, 1993.
12. Y.-I. Kim and F. Izumi, *J. Ceram. Soc. Jpn.* **102,** 401 (1994).
13. A. V. Mahajan, D. C. Johnston, D. R. Torgeson, and F. Borsa, *Phys. Rev. B* **46,** 10966 (1992).
14. N. H. Hur, S. H. Kim, K. S. Yu, Y. K. Park, J. C. Park, and S. J. Kim, *Solid State Commun.* **92,** 541 (1994).
15. H. C. Nguyen and J. B. Goodenough, *Phys. Rev. B* **52,** 324 (1995).
16. N. Menyuk, K. Dwight, and D. G. Wickham, *Phys. Rev. Lett.* **4,** 119 (1960).